Фізика аеродисперсних систем. – 2025. – № 63. – С.134-146

UDC 536.46, 533.9

Poletaev N. I.
Odessa National Maritime University, Odessa, Ukraine, E-mail: poletaev@ukr.net
ORCID: https://orcid.org/0000-0002-1340-582X

Effect of ionization in an aluminum particle dust flame on the size distribution of Al_2O_3 nanoparticles

In this review, we present the theoretical investigation results of the coagulation behavior of both neutral and thermally ionized aerosols formed by micro-dispersed aluminum combustion particles in a dust flame. A mathematical model is proposed to describe particle coagulation in both thermo-emissive and complex dusty plasma, comprising charged Al_2O_3 particles, electrons, and gas-phase ions. Particle charges were calculated using the orbital-motion-limited (OML) approximation. Ionization equilibrium in the plasma was determined by jointly solving the Saha equations for the gas phase and the charging equation for the particles. The model enabled the study of coagulation dynamics of Al_2O_3 nanoparticles. It was shown that particle charge significantly affects both the characteristic particle size and the width of the size-distribution function. In thermo-emission plasma, a strong dependence of particle size and distribution width on temperature was observed. The addition of potassium carbonate to the flame reduced the average Al_2O_3 particle size. Furthermore, increasing the concentration of the ionizing additive resulted in a narrower particle size distribution, approaching monodispersity. The results underscore the importance of accounting for Coulomb interactions in ionized systems for accurate description of the formation of condensed-phase aluminum combustion products in dust flames.

Keywords: *dust flame, micro-flame, Al_2O_3 nanoparticles, coagulation, particle size distribution, thermo-emission plasma, complex plasma, nanoparticle charge, flame ionization*

Introduction. Over the past 50 years, an extensive number of studies have been conducted worldwide on the combustion regimes and mechanisms of individual aluminum particles and their gas suspensions in various oxidizing environments. This interest is primarily driven by the potential applications of aluminum as a high-energy additive to rocket propellants, as well as by fire and explosion safety issues in industrial settings. The formation of a condensed phase during the combustion of aluminum particles has also been actively investigated to enhance the efficiency of aluminum-based fuels by reducing two-phase momentum losses in engines [1–6].

In the 1980s, at Odesa State University, method for synthesizing metal oxide nanoparticles via gas-dispersed synthesis was actively developed. This method is based on burning metal particles in laminar dust flames. The generation of such flames, their thermal and spatial structure, physical models of metal particle combustion, and the mechanisms of condensed phase formation in laminar dust flames are thoroughly discussed in [7–11].

These studies have shown that thermal ionization of both the gas and condensed components of the flame has a strong influence on the condensation of metal vapor-phase combustion products. The mechanism of this influence is associated with electrostatic interactions between charged particles, which lead to new effects not typical

DOI: 10.18524/0367-1631.2025.63.347248

of coagulation in electrically neutral aerosols [9–11]. Another, less-studied mechanism of ionization influence involves complex plasma with a high concentration of ions in the gas phase, where aerosol particles are entrained by an ion wind generated in the self-consistent electric field around charged condensed-phase particles [11–12].

The experimental and theoretical results obtained indicate the possibility of effectively controlling the characteristic size of synthesized particles through regulated ionization of the two-phase medium. At the same time, the influence of aerosol ionization on the particle size distribution in high-temperature metal flames remains virtually unexplored.

The objective of this study is to analyze the effect of thermal ionization of aluminum combustion products in a dust flame on the particle size distribution function and to determine the conditions under which narrow fractions of aluminum oxide nanopowders are formed.

1. Calculation of particle charges in the complex dusty plasma of aluminum combustion products. For the quantitative description of the charging of dust particles, two main approaches are typically used. The first is the orbital motion limited (OML) theory, and the second is the diffusion approximation.

For spherical particles with radius r_n, the condition for the applicability of the OML approach is given by the inequality:

$$r_n << \lambda_{De,Di} << l_{e,i}, \tag{1}$$

where $\lambda_{De,Di} = \sqrt{k_B T / 4\pi n_{e,i} e^2}$ is the Debye screening radius, and, $l_{e,i} = k_B T / \sqrt{2}\,\sigma_{e,i} P$ is the mean free path of electrons ($n_{e,i}$ is the concentration of electrons or ions in the gas); $\sigma_{e,i}$ is the collision cross-section of electrons or ions with neutral molecules; k_B is the Boltzmann constant; and P is the pressure.

When the condition

$$l_{e,i} << \lambda_{De,De}, r_n \tag{2}$$

is met, the diffusion charging regime approximation is used.

Since aluminum combustion in oxygen-containing environments predominantly produces aluminum oxide nanoparticles (with diameters less than 100 nm), estimates [7] show that the charging of such particles can be described using the OML approximation.

In this work, we restrict ourselves to the consideration of an equilibrium classical plasma. It is assumed that the temperatures of all plasma components and the neutral gas are equal to the combustion temperature in the microflame of an aluminum particle (T).

In the OML approximation, the flux of electrons and ions onto the surface of a particle is defined by an integral $j_{e,i} = \int \upsilon \sigma_{e,i} f_{e,i}(\upsilon) d^3\upsilon$ in which: $f_{e,i}(\upsilon)$ is the Maxwellian velocity distribution function of charged particles, $\sigma_{e,i}$ is the absorption cross-section of electrons or ions by the dust particle, $\phi_s = \dfrac{Z_n e}{4\pi\varepsilon_0 r_n}$ is the surface potential of

the particle, Z_n is the particle charge in units of the elementary charge (i.e., the charge number). For example, for thermionic emission, the integration yields:

$$j_e = -\pi \cdot r_p^2 \cdot e \cdot n_{e0} \cdot \upsilon_{Te} \cdot \begin{cases} \exp\left(-\dfrac{\phi_s \cdot e}{k_B T}\right), & \phi_s < 0 \\ \left(1 + \dfrac{\phi_s \cdot e}{k_B T}\right), & \phi_s > 0 \end{cases} \quad (3)$$

where n_{e0} is the electron concentration at a large distance from the particle ($r >> \lambda_{De}$, plasma potential $\varphi_0 = 0$), and $\upsilon_{Te} = \left(\dfrac{8k_B T}{\pi m_e}\right)^{1/2}$ is the electron thermal velocity. For an equilibrium plasma characterized by temperature T, the flux of thermoelectrons from the surface of a particle with radius r_n can be written as [4]:

$$j_T^+ = \pi r_n^2 e \cdot \nu_e \cdot \upsilon_T \cdot \exp\left(-\frac{W}{k_B T}\right) \begin{cases} 1, & \phi_s < 0 \\ \left(1 + \dfrac{\phi_s \cdot e}{k_B T}\right) \cdot \exp\left(-\dfrac{\phi_s \cdot e}{k_B T}\right), & \phi_s > 0 \end{cases} \quad (4)$$

where $\nu_e = 2\left(\dfrac{m_e k_B T}{2\pi\hbar^2}\right)^{3/2}$ is the effective density of electron states, e is the elementary charge, and W is the work function of the metal.

For a thermionic plasma in equilibrium, $\phi_s > 0$, and combining (3) and (4) gives:

$$n_{e0} = \nu_e \exp\left(-\frac{\phi_s e + W}{k_B T}\right). \quad (5)$$

For small particles ($r_n < 10$ nm), the size dependence of the electron work function must be taken into account [13]:

$$W(r_n) = W + \frac{5.40}{r_n(A)} \text{ [eV]}$$

In this equation, r_n (Å) is the particle radius in angstroms. For particles with a radius larger than 100 Å, the correction to the work function W is less than 0.05 eV.

For a thermionic dusty plasma (TP) with a number concentration of particles n_d, the charge number Z_n in the OML approximation can be determined from (5), taking into account the quasi-neutrality condition $n_{e0} = Z_n n_d$:

$$Z_n = \frac{4\pi\varepsilon_0 r_n k_B T}{e^2} \ln \frac{n_{es}}{Z_n n_d}. \quad (6)$$

where $n_{es} = \nu_e \exp\left(-W / k_B T\right)$ is the electron concentration near the surface of the particle.

In the general case, at high flame temperatures, not only the condensed phase but also the gas phase becomes ionized. The ionization of atoms and molecules with low ionization potential results in the formation of positively charged ions and free electrons (a classical example is alkali metal atoms). Atoms and molecules with high electron affinity capture free electrons and acquire a negative charge (e.g., Cl, I, AlO, AlO_2,

O_2, etc.). As a result, a complex plasma is formed, consisting of charged particles of the condensed phase, electrons, and both positive and negative gas-phase ions.

In complex plasma, the charges on the particles can be either positive ($\varphi_s > 0$) or negative ($\varphi_s < 0$). Negative charges are transferred to the particle surface by electron fluxes as described in (3), and by the total flux of all negative ions in the system:

$$j_i^- = -\pi r_n^2 e \cdot \nu_e \cdot e \sum_l Z_{il} n_{il}^- \upsilon_{Tl} \cdot \begin{cases} \exp\left(-\dfrac{\phi_s \cdot e}{k_B T}\right), & \phi_s < 0 \\ \left(1 + \dfrac{\phi_s \cdot e}{k_B T}\right), & \phi_s > 0 \end{cases} \quad (7)$$

The positive charge of the particle is maintained by thermionic emission (4) and the total flux of positive gas-phase ions onto the particle surface:

$$j_i^+ = \pi r_n^2 e \cdot \nu_e \cdot e \sum_p Z_{ip} n_{ip} \upsilon_{Tp} \cdot \begin{cases} \exp\left(-\dfrac{\phi_s \cdot e}{k_B T}\right), & \phi_s < 0 \\ \left(1 + \dfrac{\phi_s \cdot e}{k_B T}\right), & \phi_s > 0 \end{cases} \quad (8)$$

In equations (7) and (8), the subscript p refers to positive ions and l to negative ions. Z_{ip}, Z_{il} – the charge numbers of positive ($Z_{ip}>0$) and negative ions ($Z_{il}<0$), it was assumed that the ions of the gas phase were singly ionized (Z_{ip}=1 and Z_{il} = -1)

In the steady state, the sum of all fluxes is zero, i.e., the net flux vanishes. Summing the contributions of fluxes (3), (4), (7), and (8), we obtain the expression for determining the charge of aluminum oxide particles used in this study:

$$Z_n = \frac{1}{A} \cdot \begin{cases} \ln\left[\dfrac{n_{es} + \dfrac{1}{\upsilon_{Te}} \sum_p Z_{ip} n_{ip}^+ \upsilon_{Tp} \left(1 - AZ_n\right)}{n_e + \dfrac{1}{\upsilon_{Te}} \sum_l Z_{il} n_{il}^- \upsilon_{Tl}}\right] & \phi_s < 0 \\ \ln\left[\dfrac{n_{es} + \dfrac{1}{\upsilon_{Te}} \sum_p Z_{ip} n_{ip}^+ \upsilon_{Tp} \left(\dfrac{1}{1 + AZ_n}\right)}{n_e + \dfrac{1}{\upsilon_{Te}} \sum_l Z_{il} n_{il}^- \upsilon_{Tl}}\right], & \phi_s > 0 \end{cases} = \psi(n_e, n_{il}^-, n_{ip}^+, Z_n, r_n) \quad (9)$$

For convenience, a simplified notation $A = \dfrac{e^2}{4\pi\varepsilon_0 k_B T r_n}$ is introduced in equation (9). Equation (9) was used to calculate the ionization equilibrium in the microflame of an aluminum particle. For a thermionic plasma, where the ion concentrations are zero, equation (9) reduces to equation (6) under the quasi-neutrality condition $n_e = Z_n n_d$ To determine particle charges in the presence of ions in the flame, equation (9) must be solved simultaneously with the Saha equations for the gas.

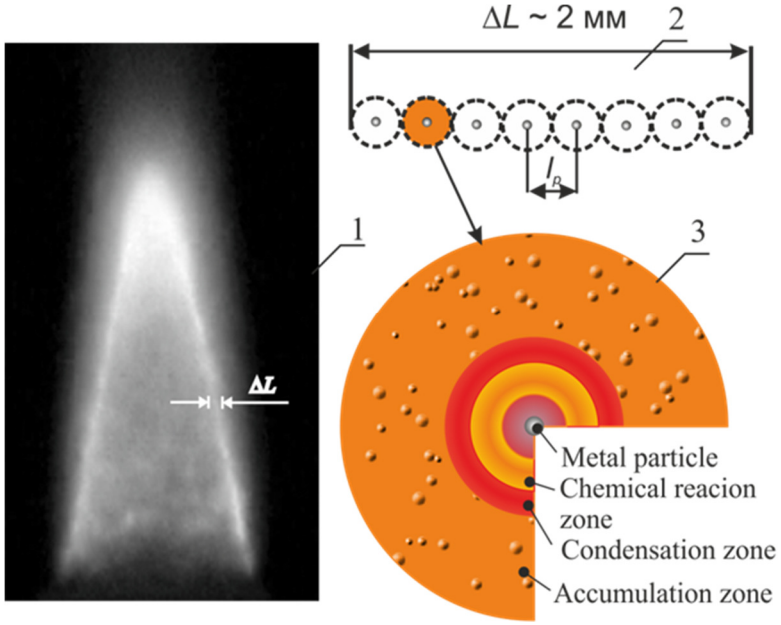

Fig. 1. Structure of the combustion zone of the flame and microflame of a metal particle: (1) laminar dust flame; (2) combustion zone; (3) microflame structure [12].

2. Model of Al_2O_3 nanoparticle coagulation in the microflame of an aluminum particle. It is known that combustion of microdispersed aluminum particles in a laminar premixed or diffusion dust flame occurs within a thin reaction zone of approximately ΔL = 1–2 mm (Fig. 1) [12]. The number concentration of monodisperse spherical fuel particles in the combustion zone is determined by the mass concentration of the metal C_f and the particle radius r_n. For a mass concentration of aluminum $C_f = 0.4$ kg/m³, particle radius $r_n = 2.4$ μm, and temperature $T = 3200$ K, accounting for thermal expansion, the number concentration of particles is approximately $n_d \approx 2 \times 10^{11}$ m^{-3}. Under these conditions, the distance between particles $l_d \approx (n_d)^{-1/3} \approx 170$ μm is much greater than the particle size. Hence, aluminum particles burn individually. This allows the combustion zone of the dust flame to be treated as a collection of independent microflames [6,12]. The microflames are under nearly identical conditions, so the description of combustion in a particle-laden gas can be reduced to the simpler model of single-particle combustion. It is convenient to assume that the volume of each microflame corresponds to the volume per metal particle, $V_d = 1/n_d$.

The microflame of a burning aluminum particle has a zonal structure, consisting of the vapor-phase combustion zone, the condensation zone, and the accumulation zone for condensed metal combustion products (Fig. 1) [12].

Reliable data on the influence of electrophysical processes on the mechanism and regime of aluminum particle combustion, as well as on their burning rate, are largely lacking. At the same time, a number of studies report results indicating a noticeable effect of flame ionization on the condensation of vapor-phase or gas-phase combustion products of microdispersed aluminum particles [1, 12, 14–16]. Models of thermionic and thermal complex plasmas in the combustion zone of dust flames for such particles are discussed in detail in [12].

The model used in the present work is based on the main assumptions of the model in [12] but differs in that it accounts for the polydispersity of aluminum oxide nanoparticles.

The size distribution of aluminum oxide nanoparticles was obtained by solving a system of kinetic equations:

$$\frac{\partial N_n}{\partial t} = \frac{1}{2}\sum_{m=1}^{n-1} k_{n-m,m} N_{n-m} N_m - N_n \sum_{m=1}^{\infty} k_{n,m} N_m \tag{10}$$

where N_n is the concentration of aluminum oxide particles in the condensation zone of the microflame, consisting of n monomer units. The first sum on the right-hand side of equation (10) represents the rate of formation of particles consisting of n monomers due to the binary coagulation process $A_{n-m} + A_m \rightarrow A_n$. The second term accounts for the loss of particles consisting of n monomers as a result of their interaction with particles of all possible sizes.

The form of the coagulation rate constant in (10) depends on the nature of the interactions between coagulating particles. Two types of interactions are considered:

1. Electrically neutral aerosol. For the free-molecular coagulation regime, the coagulation rate constant k_{nm} for neutral particles consisting of n and m monomers is given by:

$$k_{nm} = k_0 \left(n^{1/3} + m^{1/3} \right)^2 \sqrt{\frac{n+m}{n \cdot m}} \tag{11}$$

where $k_0 = \pi \cdot r_W^2 \cdot \sqrt{\frac{8 k_B T}{\pi \cdot m_g}}$, m_g is the mass of a monomer, $r_W = \left(3 m_g / 4\pi\rho\right)^{1/3}$ is the Wigner–Seitz cell radius ρ is the particle density.

2. Electrically charged particles. For charged particles, the coagulation rate constant k_{nm} has the form [10]:

$$k_{nm}^e = \begin{cases} k_{nm}\left(1 - \dfrac{U}{k_B T_g}\right), & sign(Z_n) \neq sign(Z_m) \\ k_{nm} \exp\left(-\dfrac{U}{k_B T_g}\right), & sign(Z_n) = sign(Z_m) \end{cases} \tag{12}$$

where $U(R_{\min}) = \dfrac{1}{4\pi\varepsilon_0} \dfrac{Z_m Z_n e^2}{R_{\min}}$ is the electrostatic interaction energy between particles with charge numbers Z_n and Z_m, $R_{min} = r_n + r_m$ is the minimum separation distance between particle centers.

We assume that the charges of the condensed-phase particles are of the same sign (either all positive or all negative), and that the charge can be treated as an average quantity. The applicability of these assumptions is discussed in [12].

Under these assumptions, the average particle charge is determined from equation (9):

$$Z_n = \psi(n_e, n_{il}^-, n_{ip}^+, Z_n, r_n). \tag{13}$$

Under the assumption of the existence of a local thermodynamic equilibrium in the microflame, the concentration of charged components (n_e, n_{ip}^+ and n_{il}^-) in the plasma can be estimated from the solution of p+l+1 equations of the ionization equilibrium:

$$\begin{cases} \dfrac{n_e n_{ip}^+}{(n_{ap} - n_{ip}^+)} = \dfrac{2g_{ip}}{g_{ap}} \nu_e \exp\left(-\dfrac{I_p}{k_B T_g}\right) \\ \dfrac{n_e \left(n_{al} - n_{il}^-\right)}{n_{il}^-} = \dfrac{2g_{al}}{g_{il}} \nu_e \exp\left(-\dfrac{\varepsilon_l}{k_B T_g}\right) \\ n_e = \sum_p Z_{ip} n_{ip} + \sum_l Z_{il} n_{il} + \psi(n_e, n_{il}^-, n_{ip}^+, Z_n, r_n) \sum_j r_j N_j \end{cases} \quad (14)$$

where n_{ap} – the concentration of atoms of electropositive gases (p = K, Cs, Li, Al, Na, etc.), n_{al} – the concentration of atoms of electronegative gases (l = Cl, I, AlO, AlO_2, etc.), n_{ip}^+ and n_{il}^- – the concentrations of positive and negative ions, I_p and ε_l – the ionization potentials of p-atoms and the electron affinity of l-atoms, g_{ip} and g_{il} – the degrees of degeneracy for ions, g_{ap} and g_{al} – the degrees of degeneracy for atoms of the ionizing additive, Z_{ip}, Z_{il} – the charge numbers of positive ($Z_{ip}>0$) and negative ions ($Z_{il}<0$), N_j – the concentration of Al_2O_3 particles. The first p equations and the subsequent l equations of the system (5) are Saha equations for ionization of atoms of electropositive and electronegative gases, respectively. The equation of the system for the charge numbers of particles (Z_n) and the quasi-neutrality equation complete the system of equations (14). In the calculations, it was assumed that the ions of the gas phase were singly ionized (Z_{ip}=1 and Z_{il} = -1). The ratios of the degrees of degeneracy were taken to be unity.

3. Solving the system of coagulation and ionization equilibrium equations. To solve the system of kinetic equations (10), the particle size domain was divided into sections, each represented by a characteristic volume υ_i. The volumes were chosen to satisfy the condition $\upsilon_i = 2\upsilon_{i-1}$, which allows equation (10) to be transformed into the form [17]:

$$\frac{\partial N_n}{\partial t} = N_{i-1} \sum_{m=1}^{n-2} 2^{m-n+1} k_{n-1,m} N_m + \frac{1}{2} k_{n-1,m-1} N_{n-1}^2 - N_n \sum_{m=1}^{n-1} 2^{m-n} k_{n,m} N_m - N_n \sum_{m=1}^{n_{\max}} k_{n,m} N_m \quad (15)$$

It was assumed that nuclei of the same size n_{cr} are formed in the condensation zone of the microflame, and the initial condition for equation (15) was set as: $N_1 = N_0/n_{cr}$, $N_i = 0$ for $i = 2, 3, \ldots, n_s$, where N_0 is the concentration of monomers and n_s is the number of sections in the particle size space. Based on test calculations, it can be stated that the initial size of the nuclei n_{cr} and the form of their size distribution do not affect the outcome of coagulation over time $t_{coag} > \tau_b$.

The number of sections was set to $n_s = 30$. The initial monomer concentration $N_0 = N_0(T, C_{O2})$ was determined in the approximation of an infinitely thin combustion front of aluminum vapor in oxygen [9,12].

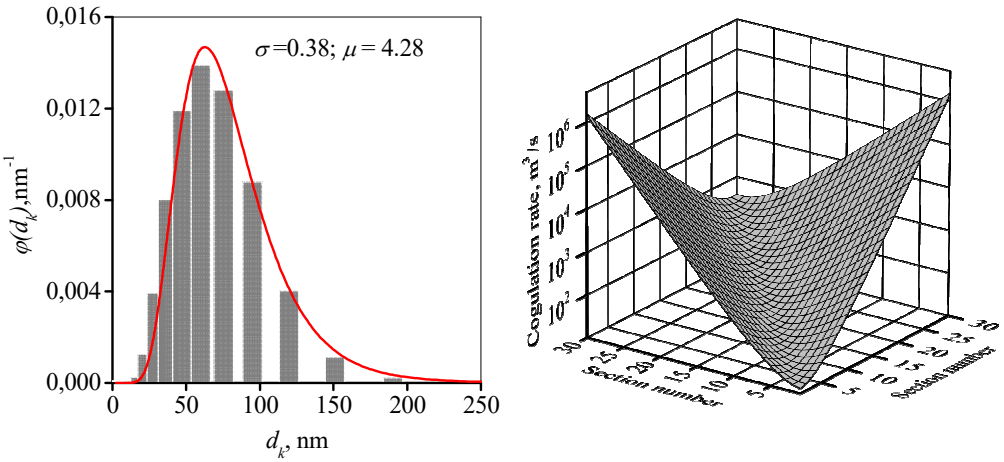

a b

Fig. 2. Size distribution function of Al_2O_3 particles (a) and dependence of the coagulation rate constant on the size of the coagulating particles (b).

Debugging and testing of the algorithm for solving (15) was performed for the coagulation of an electrically neutral aerosol in the free-molecular regime. After solving equation (15), statistical analysis was carried out to determine the main moments of the size distribution: the number average diameter (d_{10}), surface average diameter (d_{20}), volume average diameter (d_{30}), the mode (d_m), and the standard deviation s. To compare the widths of the size distributions, the coefficient of variation $Cv = \frac{s}{d_{10}} \cdot 100\%$ was calculated. Assuming a lognormal distribution of particle sizes $\phi(d) = \frac{1}{\sqrt{2\pi} d\sigma} \exp\left(-\frac{(\ln d - \mu)^2}{2\sigma^2} \right)$, the parameters of the probability density function $\mu = \ln\left(d_{10}^2 / \sqrt{s^2 + d_{10}^2} \right)$ and $\sigma = \sqrt{\ln\left(s^2 / d_{10}^2 + 1 \right)}$ were estimated.

Fig. 2a presents the solution of equation (15) with the coagulation constants from equation (11) for the combustion products of an aluminum particle (d_p = 4 μm, t_b = 2 ms) in air (C_{O2}= 0.23, T = 3100 K) and its approximation by a lognormal distribution (solid line). In all calculations, nearly all aluminum oxide particles were distributed over 8–10 sections on the size scale.

Fig. 2b shows that the coagulation rate constants ($k_{n,m} = k_{m,n}$) increase sharply when particles of large and small sizes collide. This leads to rapid absorption of small particles and causes asymmetry in the size distribution function. The minimum value of the coagulation rate constant occurs at $n = m$, and the value of $k_{n,n}$ increases monotonically with n.

4. Coagulation of aluminum oxide particles in an electron–dust plasma. The Einstein-Smoluchowski coagulation equation with rate constants of the form (11) has an analytical solution:

$$d_{30} = 3 r_W \left(k_0 N_0 t_c \right)^{2/5} \qquad (16)$$

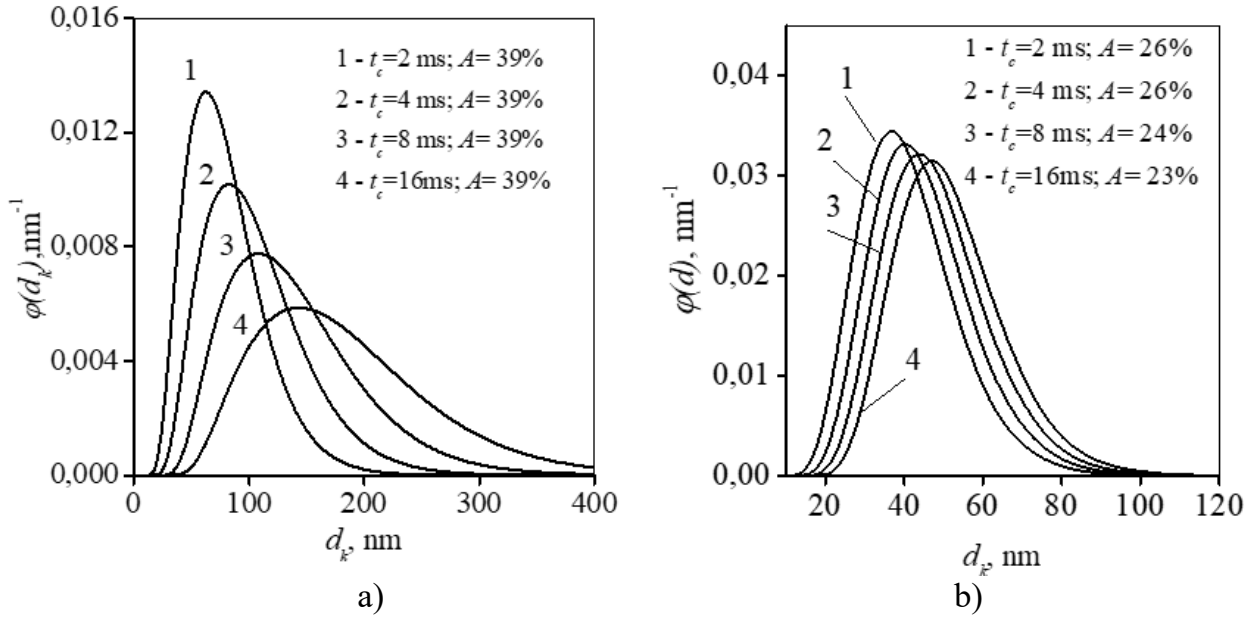

a) b)

Fig. 3. Time evolution of the size distribution function of Al_2O_3 particles for $N_0 = 2.6 \times 10^{23}\ m^{-3}$ and $T = 3000\ K$: (a) uncharged aerosol; (b) thermionic plasma.

which describes the dependence of the average cluster size on the coagulation time t_c, initial monomer concentration N_0, and the coagulation rate constant k. As seen from equation (16), these power-law dependencies are rather weak. Solving the system of equations (15) shows that in a neutral aerosol, an increase in coagulation time t_c leads to a broader size distribution function (Fig. 3a), but the coefficient of variation, which serves as a measure of aerosol polydispersity, remains unchanged ($Cv = 39\%$).

In the combustion zone of aluminum dust flames, temperatures reach 2800–3300 K. At such temperatures, nitrogen and oxygen molecules are weakly ionized. Therefore, with a low ionization potential of the metal and its oxide, a thermionic plasma (TE) is formed in the microflame, for which the quasi-neutrality condition $n_e = Z_n N_d$ holds. The coagulation rate constants for such an aerosol are given by equation (12). The calculated size distribution functions of Al_2O_3 particles in such a plasma, depending on the coagulation time, are shown in Fig. 3b.

In the ionized aerosol, the coefficient of variation becomes significantly lower (26% compared to 39% for $t_c = 2\ ms$, Fig. 3b) and decreases as coagulation time increases. The particle size distribution, as in the inert aerosol case, follows a lognormal law. The particle size depends much more weakly on the coagulation time than in the neutral aerosol. This is explained by the electrostatic repulsion between particles, which slows down the coagulation rate, especially in the region of larger aerosol particle sizes.

The calculated dependence of the average size of aluminum oxide particles (d_{10}) for ionized (TE plasma) and non-ionized (no plasma) aerosols shows a significant weakening of the dependence of the characteristic size d_{10} on coagulation time (Fig. 4). As noted earlier, for ionized aerosols, the coefficient of variation is noticeably lower than for inert aerosols and decreases with increasing coagulation time. There is also a rather strong dependence of the Al_2O_3 particle size and the coefficient of variation on the microflame temperature.

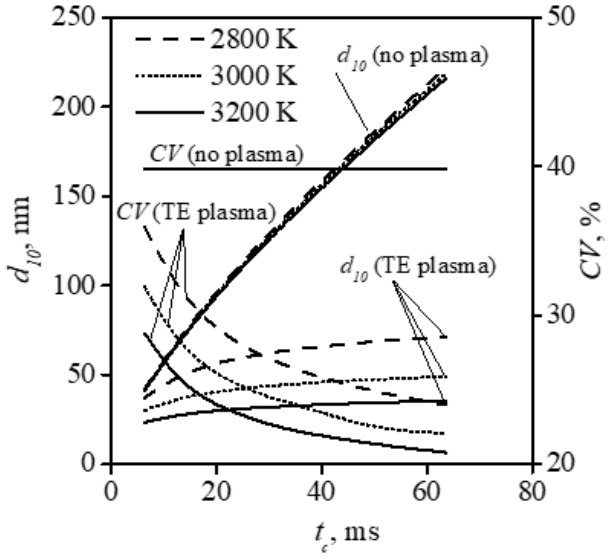

Fig. 4. Calculated dependencies of the average size d_{10} of aluminum oxide particles and the coefficient of variation Cv for neutral (no plasma) and charged (TE-plasma) aerosols. Dashed line – $T_g = 2800\ K$; dotted line – $T_g = 3000\ K$; solid line – $T_g = 3200\ K$.

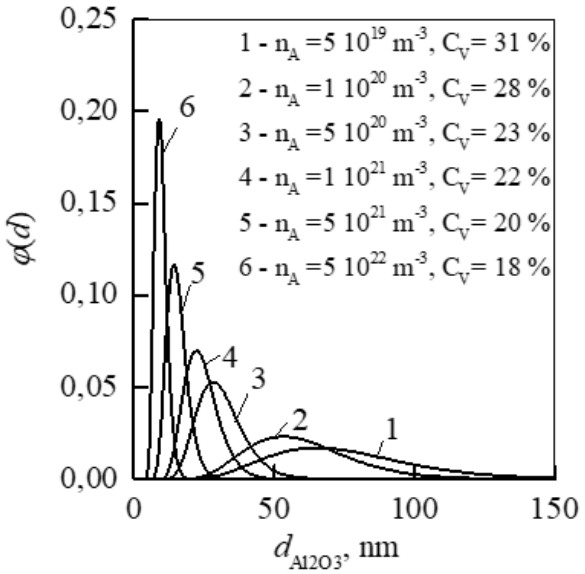

Fig. 5. Change in the Al_2O_3 particle size distribution function with potassium atom concentration.

In the temperature range $T = 2800–3200\ K$, flame ionization leads to a noticeable "splitting" in the dependencies of the average particle size and the width of their size distribution function versus temperature (Fig. 4). These differences are explained by the strong temperature dependence of the coagulation rate constant (12) for a charged aerosol.

As shown in [12], for aluminum particle flames, the existence of a pure thermionic plasma is likely an idealization. This is because, at high temperatures, the microflame contains gaseous products of condensed phase evaporation—such as atomic aluminum or various gaseous suboxides—which can acquire either a positive or negative charge.

5. Coagulation of aluminum oxide particles in electron–dust plasma with ionizing additive. The above analysis shows that in thermionic plasma, the medium temperature has a strong effect (compared to uncharged particles) on the size distribution of aluminum oxide. As the temperature increases, a more monodisperse aerosol forms (see Fig. 3b), and the average particle size decreases. However, the ability to vary the combustion temperature of aluminum is quite limited and is determined by the physicochemical properties of aluminum and its oxides.

The conditions of ionization equilibrium in the microflame can be significantly altered by introducing atoms with low ionization potential or high electron affinity into the combustion zone [7, 11, 12]. Calculations show high effectiveness of this approach for synthesizing nearly monodisperse aluminum oxide particles with diameters down to 5–10 nanometers (Fig. 5). Calculations were performed for Al particles $d_{10} = 5\ \mu m$, $T = 3200\ K$, $C_{O2} = 0.23$. As the potassium atom concentration varied from 5×10^{19} m^{-3}

(below which the distribution function ceased to change) to 5×10^{22} m^{-3}, the average particle size decreased from 72 nm to 9.3 nm. At the same time, the particles became more monodisperse, as evidenced by a decrease in the coefficient of variation from 31% to 18%.

This method of increasing the dispersion of aluminum oxide nanoparticles was experimentally studied in [7, 11]. It was found that when potassium carbonate was used as the ionizing additive, the dependence of the characteristic particle size on potassium concentration exhibited a minimum. In a later work [12], this extremal behavior was confirmed for cesium and iodine atoms. For monodisperse aerosol, this effect was analyzed in detail in [7, 12]. However, a complete understanding of the extremal dependence of Al_2O_3 particle size on the concentration of ionizing impurities is still lacking.

Conclusions. The studies conducted show that thermal ionization in the combustion zone of aluminum dust flames plays an important role in the formation of condensed aluminum combustion products. For unipolarly charged particles, electrostatic repulsion significantly slows down the coagulation rate, leading to smaller characteristic particle sizes and narrower size distribution functions compared to classical coagulation. Moreover, longer coagulation times correspond to narrower distribution functions. The spread of distribution modes for different coagulation times is also significantly smaller for charged aerosols than for uncharged ones.

Temperature in the condensation zone of the microflame becomes a significant parameter influencing the dispersion of combustion products. This feature strongly distinguishes plasma coagulation from that in uncharged aerosols and may be useful for smoke plasma diagnostics or controlling the dispersion of aluminum combustion products.

The most pronounced effect on aluminum oxide nanoparticle dispersion is achieved through flame ionization with alkali metal atoms. As the concentration of the ionizing additive increases, the particle size distribution becomes increasingly narrow, approaching a monodisperse form. The results obtained lead to the conclusion that to adequately describe the formation processes of the condensed phase of aluminum combustion products, it is necessary to account for flame thermal ionization.

References

1. *V.E. Zarko, O.G. Glotov* Formation of Al oxide particles in combustion of aluminized condensed systems (review) // Sci. Technol. Energ. Mater. – 2013. – Vol. 74 (6). – P. 139–143.
2. *Oleg G. Glotov, Vladimir E. Zarko* Chapter Eleven - Formation of Nanosized Products in Combustion of Metal Particles // Energetic Nanomaterials Synthesis, Characterization, and Application. – 2016, P. 285-321.
3. *Valery A. Babuk, Nikita L. Budnyi*. Smoke oxide particles formation at the burning surface of condensed systems // Acta Astronautica. – 2019. – 158. 264–271.
4. *V. Karasev, A. A. Onishchuk, S. A. Khromova, O. et al.* Formation of Metal Oxide Nanoparticles in Combustion of Titanium and Aluminum Droplets //Combust., Expl., Shock Waves. –2006. – 42 (6), 471–476.

5. *D. A. Yagodnikov and E. I. Gusachenko*, Experimental Study of the Disperse Composition of Condensed Products of Aluminum-Particle Combustion in Air // Combust., Expl., Shock Waves. – 2004. – 40 (2), 154–162.
6. *A. N. Zolotko, Ya. I. Vovchuk, N. I. Poletayev, A. V. Florko, and I. S. Altman.* Synthesis of Nanooxides in Two-Phase Laminar Flames //Combust., Expl., Shock Waves. – 1996. – 32 (3), 262–269.
7. *A. N. Zolotko, N. I. Poletaev, and Ya. I. Vovchuk.* Gas-Disperse Synthesis of Metal Oxide Particles // Combust., Expl., Shock Waves. – 2015. – 51 (2), 252–268.
8. *N. I. Poletaev, A. N. Zolotko, and Yu. A. Doroshenko*. Degree of Dispersion of Metal Combustion Products in a Laminar Dust Flame // Combust., Expl., Shock Waves. – 2011. – 47 (2), 153-165.
9. *N. I. Poletaev.* Formation of Condensed Combustion Products in Metal Dust Flames: Nucleation Stage // Combust., Expl., Shock Waves. – 2015. – 51 (3), 299-312.
10. *N. I. Poletaev.* Formation of Condensed Combustion Products in Metal Dust Flames: Coagulation Stage //Combust., Expl., Shock Waves. – 2015. – 51 (4), 444–456.
11. *N. I. Poletaev and Yu. A. Doroshenko* Effect of Addition of Potassium Carbonate to Aluminum Powder on the Grain Size of Al_2O_3 Nanoparticles Formed in the Laminar Dusty Flame // Combust., Expl., Shock Waves. – 2013. – 49 (1), P. 26–37.
12. *Poletaev N.I., Khlebnikova M.E.* Coagulation of the Ionized Combustion Products in a Dust Flame of Aluminum Particles // Journal of Chemistry. – 2019. Article ID 4753910.
13. *B. M. Smirnov*, Cluster Plasma // Usp. Fiz. Nauk. – 2000. – 170 (5), 495–534.
14. *Alexander M. Savel'ev and Dmitriy A. Yagodnikov* Mechanism of Electric Charging of Aluminum Oxide Particles When Burning Solid Fuels // Journal of Propulsion and Power,2022, 38:5, pp. 771–782
15. *Xiong, Y., Pratsinis, S. E., & Mastrangelo, S. V.* The effect of ionic additives on aerosol coagulation // Journal of colloid and interface science. – 1992. – 153(1), 106–117.
16. *J.A. Doroshenko, N.I. Poletaev, V.I. Vishnyakov.* Dispersion of dust sizes in the plasma of aluminum dust flame // Phys. Plasmas. – 2009. – 16, 094504.
17. *M. J. Hounslow, R. L. Ryall, V. R. Marshall.* A discretized population balance for nucleation, growth, and aggregation // AIChE Journal. 1988. – V. 34, Issue11. – P. 1821-1832.

Фізика аеродисперсних систем. – 2025. – № 63. – С.134-146

М.І. Полєтаєв

Вплив іонізації в пиловому полум'ї частинок алюмінію на розподіл наночастинок Al_2O_3 за розмірами

У цій роботі представлено результати теоретичних досліджень коагуляції як нейтрального, так і термічно іонізованого аерозолю, що утворюється в результаті згоряння мікродисперсних частинок алюмінію в пиловому полум'ї. Запропоновано математичну модель коагуляції частинок у термоемісійній та комплексній пиловій плазмі, що включає заряджені частинки Al_2O_3, електрони та іони газової фази. Заряд наночастинок був розрахований в наближенні обертально-обмеженого руху (OML). Іонізаційна рівновага в плазмі визначалася спільним вирішенням рівнянь Саха для газової фази та рівняння заряджання частинок. Модель дозволила вивчити динаміку коагуляції наночастинок Al_2O_3. Показано, що заряд частинок суттєво впливає на характерний розмір частинок та ширину функції розподілу за розмірами. У термоемісійній плазмі виявлено значну залежність розмірів частинок і ширини розподілу від температури. Додавання карбонату калію в полум'я зменшило середній розмір частинок Al_2O_3. Збільшення концентрації іонізуючої добавки призводить до звуження розподілу частинок за розмірами, наближаючи його до монодисперсного. Отримані результати підкреслюють важливість врахування кулонівських взаємодій в іонізованій системі для адекватного опису процесів формування конденсованої фази продуктів горіння алюмінію в пилових полум'ях.

Ключові слова: *пилове полум'я, мікрополум'я, наночастинки Al_2O_3, коагуляція, розподіл частинок за розмірами, термоемісійна плазма, комплексна плазма, заряд наночастинок.*